Exploration of Targeted Anti-tumor Therapy

Open Exploration

Open Access Original Article

Anti-angiogenic effects of *Moringa oleifera* silver nanoparticles on endothelial cells: in vitro and ex vivo studies

Rolla Al-Shalabi[1,2], Vuanghao Lim[1], Ibrahim Al-Deeb[3], Melissa Kilus[1], Nozlena Abdul Samad[1*]

[1]Department of Toxicology, Advanced Medical and Dental Institute, Sains@BERTAM, Universiti Sains Malaysia, Kepala Batas 13200, Pulau Pinang, Malaysia

[2]Pharmacological and Diagnostic Research Center, Al-Ahliyya Amman University, Al-Salt 19628, Jordan

[3]Faculty of Pharmacy, Zarqa University, Zarqa 13132, Jordan

***Correspondence:** Nozlena Abdul Samad, Department of Toxicology, Advanced Medical and Dental Institute, Sains@BERTAM, Universiti Sains Malaysia, Kepala Batas 13200, Pulau Pinang, Malaysia. nozlena@usm.my

Academic Editor: Katrin Sak, NGO Praeventio, Estonia

Received: April 16, 2025 **Accepted:** June 23, 2025 **Published:** July 27, 2025

Cite this article: Al-Shalabi R, Lim V, Al-Deeb I, Kilus M, Abdul Samad N. Anti-angiogenic effects of *Moringa oleifera* silver nanoparticles on endothelial cells: in vitro and ex vivo studies. Explor Target Antitumor Ther. 2025;6:1002332. https://doi.org/10.37349/etat.2025.1002332

RETRACTED ARTICLE

Abstract

Aim: Angiogenesis, invasion, and tube formation are critical processes in tumor progression and metastasis. The use of nanoparticles derived from natural products presents a promising approach for targeted cancer therapy. This study evaluates the anti-angiogenic and anti-invasive effects of *Moringa oleifera* silver nanoparticles (MO-AgNPs) as a therapeutic strategy against these processes.

Methods: The anti-angiogenic and anti-invasive activities of MO-AgNPs were investigated using a series of in vitro and ex vivo models. These included the rat aortic ring assay, endothelial tube formation assay, cell invasion assay using endothelial cell lines (Ea.hy926), and a three-dimensional (3D) co-culture spheroid model to simulate tumor microenvironment behavior. Comparisons were made with known inhibitors: quercetin (15.11 µg/mL) and suramin (100 µg/mL).

Results: MO-AgNPs at 12 µg/mL significantly inhibited Ea.hy926 cell invasion by 62.10% and significantly suppressed endothelial tube formation, comparable to the effect of quercetin. In the ex vivo aortic ring assay, MO-AgNPs reduced microvessel sprouting by 83.824 ± 0.081%, surpassing the inhibition achieved by suramin. Additionally, in the 3D spheroid model, MO-AgNPs at concentrations of 12 µg/mL and 6 µg/mL, as well as quercetin, significantly reduced spheroid diameter by day 14, indicating suppressed invasive potential and angiogenic support.

Conclusions: MO-AgNPs exhibit strong anti-angiogenic and anti-invasive effects across various tumor-relevant models, highlighting their potential as a therapeutic agent against tumor progression and angiogenesis-related diseases. These results support further investigation of MO-AgNPs as a novel nanotherapeutic for cancer treatment.

© The Author(s) 2025. This is an Open Access article licensed under a Creative Commons Attribution 4.0 International License (https://creativecommons.org/licenses/by/4.0/), which permits unrestricted use, sharing, adaptation, distribution and reproduction in any medium or format, for any purpose, even commercially, as long as you give appropriate credit to the original author(s) and the source, provide a link to the Creative Commons license, and indicate if changes were made.

Keywords

Anti-angiogenic effects, endothelial cells, ex vivo, in vitro, *Moringa oleifera* silver nanoparticles

Introduction

Moringa oleifera, commonly referred to as the "drumstick tree" or "miracle tree", is a multipurpose plant known for its high nutritional value and broad-spectrum therapeutic properties. Traditionally used in various cultures as both a food source and natural remedy, it contains a rich array of essential nutrients, vitamins, minerals, and bioactive compounds, contributing to its role in supporting health and addressing malnutrition [1, 2]. Specifically, *Moringa oleifera* leaf extract was utilized as both a reducing and stabilizing agent, which contains a diverse array of bioactive compounds such as flavonoids, phenolic acids, and alkaloids. These phytochemicals play a critical role in the reduction of silver ions and capping of nanoparticles, thereby influencing the physicochemical properties and biological activity of *Moringa oleifera* silver nanoparticles (MO-AgNPs) [3]. While the exact composition of bioactive molecules adsorbed onto the nanoparticles can vary depending on extraction and synthesis conditions, studies have shown that flavonoids and phenolics are predominantly responsible for the observed antioxidant and anti-inflammatory effects, which likely contribute to the anti-angiogenic activity demonstrated in our results. Recent advances in nanotechnology have enabled the development of MO-AgNPs, which are gaining attention for their potential biomedical applications. This study investigates the effects of MO-AgNPs on angiogenesis, metastasis, and vascular development, biological processes central to tumor progression and dissemination. Angiogenesis, the formation of new blood vessels from pre-existing vasculature, is a hallmark of cancer that supports tumor growth and metastasis. The metastatic cascade further involves cancer cell invasion, migration, and interaction with the tumor microenvironment [4, 5].

To evaluate the anti-angiogenic and anti-metastatic properties of MO-AgNPs, a series of in vitro and ex vivo assays were conducted, including endothelial tube formation, cancer cell invasion, three-dimensional (3D) spheroid formation, and rat aortic ring assays. The tube formation assay models angiogenesis by assessing capillary-like structure formation by endothelial cells (ECs). Invasion assays quantify the ability of cancer cells to penetrate extracellular matrices in response to nanoparticle treatment. The ex vivo aortic ring assay provides insight into the effects of MO-AgNPs on microvessel sprouting and endothelial dynamics. The 3D spheroid model mimics in vivo tumor architecture, enabling evaluation of nanoparticle-induced changes in tumor growth and viability within a physiologically relevant context.

This study aims to elucidate the mechanistic impact of MO-AgNPs on angiogenesis and metastasis, offering insights into their potential as targeted anti-tumor agents. The findings contribute to the growing body of research on nanoparticle-based strategies for cancer therapy.

Materials and methods

Preparation and green synthesis of MO-AgNPs

Leaves of *Moringa oleifera* were subjected to sequential extraction using absolute ethanol, 50% ethanol, and deionized water. Briefly, 25 g of dried leaf powder was extracted with 250 mL of absolute ethanol (1:10 w/v), sonicated for 30 minutes, and centrifuged at 6,000 rpm for 15 minutes. The extraction was repeated twice, and the pooled supernatants were filtered and concentrated using a rotary evaporator at 60˚C. The extract was stored at 4˚C. The remaining pellet was re-extracted sequentially with 50% ethanol and deionized water using the same procedure. The final aqueous extract was lyophilized and stored at 4˚C for further use.

Green synthesis of MO-AgNPs was carried out by mixing 10 mL of 1% (w/v) aqueous extract with 90 mL of 169.88 µg/mL silver nitrate ($AgNO_3$) solution. The reaction mixture was incubated at 60˚C for 8 h under continuous agitation. Nanoparticle formation was indicated by a color change from yellowish to dark brown. The synthesized nanoparticles were collected by centrifugation at 6,000 rpm for 30 minutes, washed three times with deionized water, freeze-dried, and stored at 4˚C until use [6].

RETRACTED ARTICLE

Nanoparticle characterization

Basic physicochemical characterization of the synthesized nanoparticles was performed using ultraviolet-visible (UV-Vis) spectroscopy, dynamic light scattering (DLS), and zeta potential analysis. As the DLS and zeta potential data have been previously published in our earlier work [7], UV-Vis spectroscopy data are included in Figure S1.

Assessment of EC invasion

To investigate the anti-invasive potential of MO-AgNPs as a targeted anti-tumor therapy, this study assessed their ability to inhibit the invasion of the EC line (Ea.hy926) through a Matrigel® barrier (Corning, USA) [8, 9]. Matrigel, diluted in Dulbecco's modified eagle medium (DMEM) at a 1:1 ratio, was dispensed into a 96-well plate and allowed to solidify for 1 h. Subsequently, 5,000 cells per well were seeded and treated with one of the following: 0.05% DMSO:0.05% deionized water (negative control), 15.11 µg/mL quercetin (Genochem World, Spain) as a positive control, or MO-AgNPs at concentrations of 12, 6, 3, and 1.5 µg/mL.

The plates were incubated for 24 h at 37˚C in a humidified atmosphere containing 5% CO_2. Following incubation, the upper medium containing non-invaded cells was gently removed, and wells were washed with phosphate buffered saline (PBS). The number of invaded cells remaining in the lower matrix was quantified using an inverted microscope at 40× magnification [10].

The degree of invasion inhibition was calculated by averaging cell counts from multiple microscopic fields and applying the following formula:

$$Cell\ invasion\ inhibition\ (\%) = \left[\frac{1 - (Average\ cells\ invading\ Matrigel\ in\ treated\ group) \times 100}{Average\ cells\ invading\ Matrigel\ in\ untreated\ group}\right]$$

Three independent experiments were conducted, and the results were presented as mean ± standard deviation (SD).

Tube formation assay for ECs

This assay was conducted to evaluate the inhibitory effects of MO-AgNPs on the ability of Ea.hy926 cells to form capillary-like structures on Matrigel® [11, 12]. Ea.hy926 cells were first cultured in flasks for 48 h. After this incubation period, the culture medium was replaced with fresh DMEM containing either 0.05% DMSO:0.05% deionized water (negative control), 15.11 µg/mL quercetin (positive control), or MO-AgNPs at concentrations of 12, 6, 3, and 1.5 µg/mL.

Following 24 h of treatment, Matrigel diluted 1:1 with DMEM was added to each well of a 48-well plate and allowed to solidify for one hour. Cells from the treated flasks were then counted, and 100,000 cells were resuspended in fresh DMEM and seeded into each well. The formation of tube-like structures was monitored at two-hour intervals under an inverted microscope, with typical tube formation observed approximately two and a half hours post-seeding. Images were captured at 40× magnification using an Olympus CKX41 digital camera (Japan).

The percentage of inhibition of tube formation was calculated using the following formula:

$$Tube\ formation\ inhibition\ (\%) = \left[\frac{1 - (Average\ of\ enclosed\ area\ in\ treated\ group) \times 100}{Average\ of\ enclosed\ area\ in\ untreated\ group}\right]$$

Ex vivo anti-angiogenic evaluation using rat aortic ring assay

The ex vivo rat aortic ring assay was employed to assess the anti-angiogenic potential of MO-AgNPs. This 3D assay is widely regarded as one of the most effective models for studying angiogenesis. Modifications were applied to the standard protocols originally described by Rahman et al. [13], Aplin and Nicosia [14, 15] to optimize the procedure for this study.

Experimental animals

Male Wistar rats, weighing approximately 200 g, were housed under a controlled 12 h light/dark cycle at 25 ± 2˚C with regulated humidity. All animal care and experimental procedures strictly complied with the USM

RETRACTED ARTICLE

Institutional Animal Care and Use Committee (IACUC) guidelines and received ethical approval under reference number USM/IACUC/2022/(137)(1230).

Culturing rat aortic rings

Rats were humanely euthanized via cervical dislocation following CO_2 inhalation to ensure death. The thoracic aorta was carefully excised and immediately immersed in M199 medium to preserve its structural integrity. The aorta was then sectioned into uniform rings and individually placed into the wells of a 48-well plate (Costar Corning, USA). After the lower matrix layer had solidified, 10 µL of thrombin (50 U/mL, Sigma-Aldrich, USA) in normal saline containing bovine serum albumin was added to each well. The plate was incubated for 1.5 h at 37˚C in a humidified incubator with 5% CO_2 to facilitate matrix polymerization and initial tissue stabilization [16].

Culture medium

M199 medium (Gibco/Life Technologies, USA) was used as the base growth medium. The assay was performed using two freshly prepared layers. The lower layer consisted of M199 medium mixed with fibrinogen (Merck, Germany), L-glutamine (Gibco/Life Technologies, USA), and aprotinin (Sigma-Aldrich, USA). The upper layer contained M199 medium supplemented with fetal bovine serum (FBS), ε-aminocaproic acid (Sigma-Aldrich, USA), L-glutamine, amphotericin B (Lonza Group Ltd., Switzerland), gentamicin, and penicillin-streptomycin.

Rat aortic rings treatment

After incubation, MO-AgNPs were added to the upper layer of each well at concentrations of 12, 6, 3, and 1.5 µg/mL. Suramin (100 µg/mL; Sigma-Aldrich, USA) served as the positive control, while 0.05% DMSO mixed with 0.05% deionized water was used as the negative control. The plates were then incubated at 37˚C in a 5% CO_2 atmosphere for seven days. On the fourth day, the medium in the upper layer was replaced with fresh M199 medium containing the same treatment concentrations. Neovascularization was evaluated using an inverted microscope at 40× magnification, equipped with a digital camera.

Quantification and evaluation of neovascularization

Microvessel outgrowth was measured to assess neovascularization, following the method described by Nicosia [15] and Kapoor et al. [17]. Images were analyzed using Motic Image Plus Version II software (Motic China Group Co., Ltd.). The percentage of neovascularization inhibition was calculated using the following formula:

$$Neovasularization\ inhibition\ (\%) = \left[100 \times \left(1 - \frac{A_0}{A}\right)\right]$$

where A_0 is the distance of blood vessel growth in the sample, and A is the distance of blood vessel growth in the control. Results were presented as mean ± SD.

Hanging drop spheroids model for co-culturing EA.hy926 and HT29 cells

Formation of spheroid

Approximately 1.25×10^5 cells from each of the EA.hy926 and HT29 cell lines were suspended in 1 mL of complete DMEM medium containing 1% D-glucose (Sigma-Aldrich, USA). From this suspension, 20 µL containing 5×10^3 cells of each cell line was carefully pipetted onto the inner surface of a 6-well plate cover. The plate cover was then gently inverted and placed over a 6-well plate containing 2 mL of DMEM in each well to prevent dehydration. The plates were incubated for 72 h, during which spheroid formation was monitored using a dissecting microscope. Once the spheroids had developed, one spheroid from each well was transferred into a 96-well plate. Each well contained 50 µL of a pre-mixed Matrigel and DMEM solution at a 1:1 ratio. Using a pipette, the spheroids were carefully placed on top of the solidified Matrigel, followed by the addition of 100 µL fresh DMEM. The plate was then incubated for 1 h to allow the spheroids to settle [18].

RETRACTED ARTICLE

Treatment of spheroids with MO-AgNPs

After a 1 h incubation, 100 µL of MO-AgNPs at concentrations of 1.5, 3, 6, and 12 µg/mL were added to each well. Quercetin (15.11 µg/mL) served as the positive control, while 0.05% DMSO combined with 0.05% deionized water was used as the negative control. The plates were then incubated for 14 days. Images of each spheroid were captured at days 0, 3, 8, and 14 using an inverted microscope at 40× magnification. The surface area and diameter of the spheroids were measured using Motic software version 2 (Motic China Group Co., Ltd.). Results are presented as mean ± SD. The volume of each spheroid from day 0 to 14 was calculated using the following equation:

$$Volume\ of\ spheroid = 4/3 \times \pi \times Radius\ of\ spheriod^3$$

The growth percentage of spheroids at any given time point was normalised to the negative control using the following formula:

$$Spheroid\ growth\ (\%) = \left(\frac{Average\ volume\ of\ spheroid\ in\ treated\ group}{Average\ volume\ of\ spheroid\ in\ untreated\ group}\right) \times 100$$

Statistical data analysis

Data are presented as mean ± SD. Statistical significance was indicated by * for *P*-values less than 0.05 and ** for *P*-values less than 0.01. The non-parametric Kruskal-Wallis test, which is equivalent to ANOVA, was used to assess significant differences. All analyses were performed using SPSS version 22.0 (SPSS Inc., Chicago, IL) [19].

Cell line source, authentication, and contamination testing

The Ea.hy926 and the colorectal cancer cell line HT29 were obtained from the American type culture collection (ATCC). Both cell lines were authenticated using short tandem repeat (STR) profiling prior to experimentation to confirm their identity and ensure the absence of cross-contamination with other cell lines. STR profiling was conducted by ATCC following their standard protocols. Additionally, all cell cultures used in this study were confirmed to be free from mycoplasma contamination.

Results

Preparation and synthesis of MO-AgNPs

Moringa oleifera leaves were sequentially extracted using ethanol, 50% ethanol, and distilled water. Among these, the aqueous extract characterized by its yellowish color and dry, flaky texture was chosen for nanoparticle synthesis due to its high solubility and rich bioactive content. For the synthesis of MO-AgNPs, the water-soluble extract was mixed with a 169.88 µg/mL $AgNO_3$ solution. The mixture was incubated in a water bath at 60˚C with continuous agitation for 8 h. A visible color change from clear yellow to dark brown indicated the successful reduction of Ag^+ ions and formation of silver nanoparticles.

Characterization of MO-AgNPs

The successful synthesis of MO-AgNPs was confirmed using UV-Vis spectroscopy, DLS, and zeta potential analysis. UV-Vis spectroscopy showed a characteristic absorption peak at approximately 430 nm, indicating the formation of silver nanoparticles. The UV-Vis spectroscopy results are provided in Figure S1. In our previous study, we observed that DLS analysis revealed an average particle size of 57.88 nm and a polydispersity index (PDI) of 0.475, indicating moderate size uniformity. The zeta potential value was −15.9 mV, suggesting moderate colloidal stability and reduced nanoparticle aggregation. These results confirm that the green synthesis method successfully produced stable and well-dispersed nanoparticles suitable for biological applications [7].

Invasion inhibition in in vitro human ECs by MO-AgNPs

The anti-invasive effect of MO-AgNPs on Ea.hy926 was assessed using concentrations of 12, 6, 3, and 1.5 µg/mL over a 24 h period. Quercetin (15.11 µg/mL) served as the positive control, while a 0.05% DMSO:0.05% deionized water solution was used as the negative control. The results revealed a significant

RETRACTED ARTICLE

reduction in the number of cells invading the Matrigel® matrix in all MO-AgNP-treated groups compared to the untreated control (Figures 1 and 2). The number of invaded cells per mm^2 was 34.67 ± 1.25, 36.33 ± 1.25, 45.33 ± 1.25, and 57.33 ± 1.25 for the 12, 6, 3, and 1.5 µg/mL MO-AgNP treatments, respectively. In comparison, quercetin treatment resulted in 39.67 ± 1.25 cells/mm^2, while the negative control showed 91.67 ± 2.05 cells/mm^2. The calculated invasion inhibition rates for MO-AgNPs were 62.10%, 60.40%, 50.50%, and 37.50% at 12, 6, 3, and 1.5 µg/mL, respectively. Notably, the 12 µg/mL MO-AgNP treatment demonstrated a comparable inhibitory effect (62.10%) to that of quercetin (56.70%) (Figure 3).

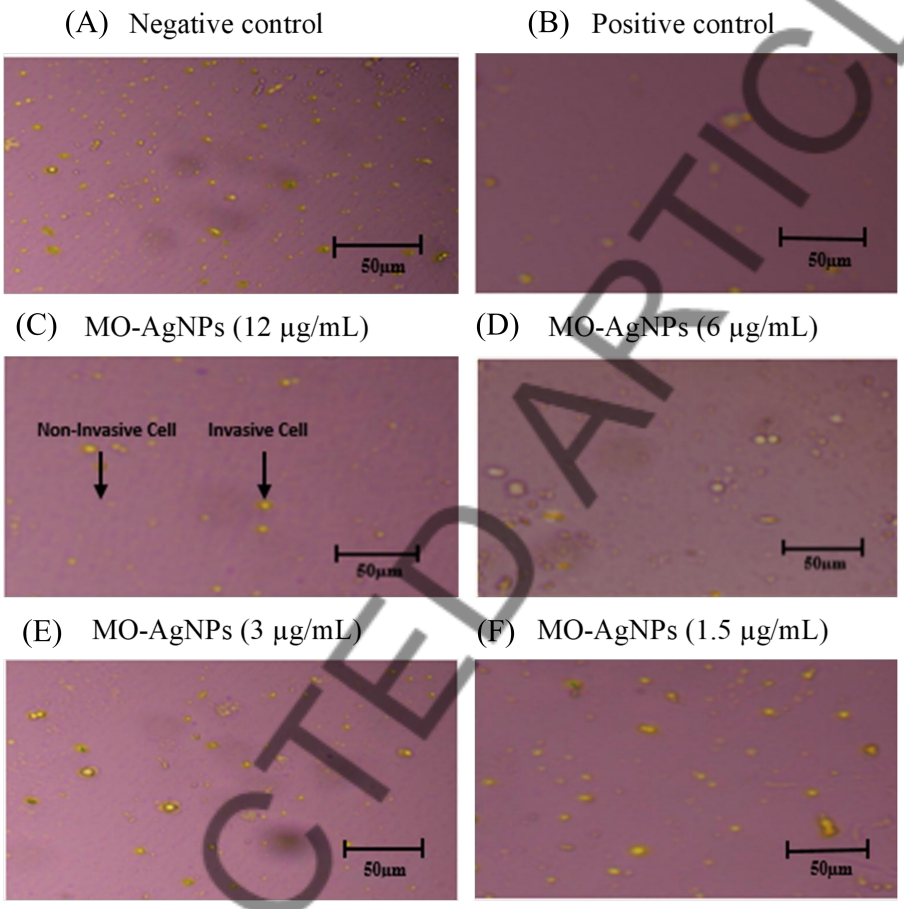


Figure 1. Inhibitory effect of MO-AgNPs on the invasion of Ea.hy926. Images captured under an inverted microscope at 40× magnification illustrate the extent of invasion by Ea.hy926 cells following treatment with graded concentrations of MO-AgNPs. Cells were exposed to: (**A**) negative control (0.05% DMSO:0.05% deionized water); (**B**) positive control (quercetin, 15.11 µg/mL); (**C**) MO-AgNPs at concentrations of 12 µg/mL; (**D**) MO-AgNPs at concentrations of 6 µg/mL; (**E**) MO-AgNPs at concentrations of 3 µg/mL; (**F**) MO-AgNPs at concentrations of 1.5 µg/mL. A concentration-dependent reduction in cell invasion was observed, suggesting that MO-AgNPs possess anti-invasive properties against human endothelial cells. MO-AgNPs: *Moringa oleifera* silver nanoparticles; Ea.hy926: endothelial cell line

Endothelial tube formation inhibition by MO-AgNPs

The ability of Ea.hy926 to form tube-like structures, an essential step in angiogenesis, was evaluated in the presence of MO-AgNPs. Treatment with MO-AgNPs at concentrations of 12 and 6 µg/mL resulted in nearly 100% inhibition of tube formation compared to the negative control. These inhibitory effects were also comparable to those observed with the positive control, quercetin (15.11 µg/mL). According to Almatroodi et al. [20], quercetin at low concentrations (15.11 µg/mL) exhibits significant antiangiogenic activity, supporting its suitability as a positive control in this study.

Images were captured after 2.5 h of incubation. No closed tubular structures were observed in the MO-AgNP-treated groups during this period. Interestingly, untreated ECs aggregated and formed a prominent tube-like structure by 2.5 h (Figure 4). In contrast, MO-AgNP-treated cells showed complete inhibition of tube formation at all tested concentrations.

RETRACTED ARTICLE

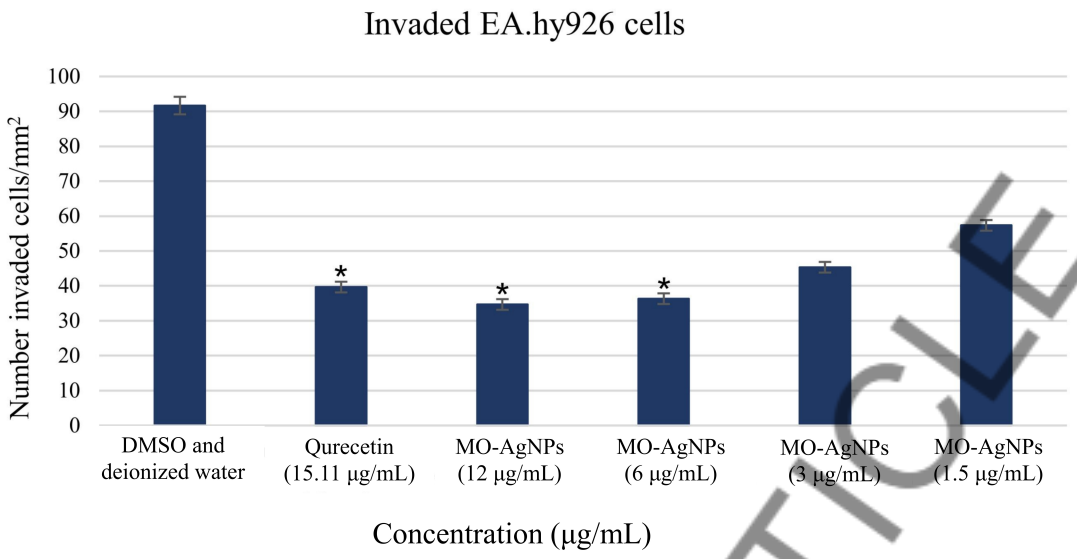


Figure 2. Quantification of invaded Ea.hy926 cells through Matrigel® following 24 h treatment with MO-AgNPs. The number of invaded cells per mm^2 was assessed after treatment with MO-AgNPs at concentrations of 12, 6, 3, and 1.5 µg/mL, compared to a positive control (quercetin, 15.11 µg/mL) and a negative control (0.05% DMSO:0.05% deionized water). Results are expressed as the mean number of invaded cells per mm^2. Statistical analysis was performed using the Kruskal-Wallis test. * *P*-value < 0.05 indicates statistically significant differences compared to the negative control. Ea.hy926: endothelial cell line; MO-AgNPs: *Moringa oleifera* silver nanoparticles

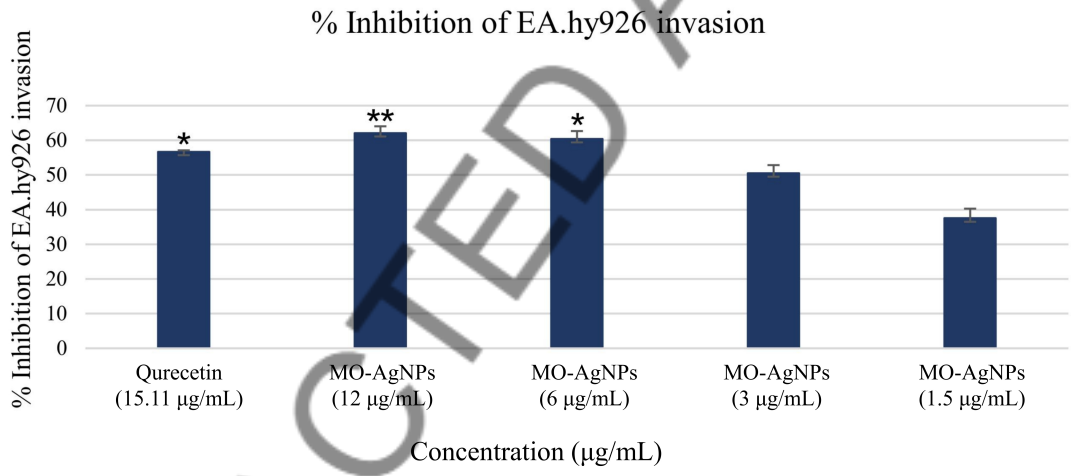


Figure 3. Inhibition percentage of Ea.hy926 cell invasion following treatment with MO-AgNPs and quercetin. The percentage of invasion inhibition was calculated by normalizing treated groups against the negative control (0.05% DMSO:0.05% deionized water). Treatments included MO-AgNPs at concentrations of 12, 6, 3, and 1.5 µg/mL, as well as quercetin (15.11 µg/mL) as a positive control. Statistical significance was determined using the Kruskal-Wallis test. **P*-value < 0.05, ***P*-value < 0.01 indicate significant differences compared to the negative control. Ea.hy926: endothelial cell line; MO-AgNPs: *Moringa oleifera* silver nanoparticles

Measuring neovascularization formation inhibition of MO-AgNPs by ex vivo rat aortic ring assay

The ex vivo rat aortic ring assay was conducted to assess the anti-angiogenic properties of MO-AgNPs. At a concentration of 12 µg/mL, MO-AgNPs exhibited the highest level of neovascularization inhibition, achieving 83.824 ± 0.081%, which surpassed the inhibition observed with the positive control, suramin (100 µg/mL), at 70.927 ± 0.703% (Figure 5). The inhibition rates for MO-AgNPs at concentrations of 6, 3, and 1.5 µg/mL were 72.065 ± 0.657%, 23.321 ± 0.563%, and 13.599 ± 0.755%, respectively (Table 1, Figure 6). Statistical analysis revealed that MO-AgNPs treatments at 12 and 6 µg/mL significantly inhibited neovascularization compared to the negative control (*P*-value < 0.01). These findings demonstrate that MO-AgNPs exert strong anti-angiogenic effects in a dose-dependent manner, highlighting their potential as therapeutic agents for angiogenesis-related diseases.

RETRACTED ARTICLE

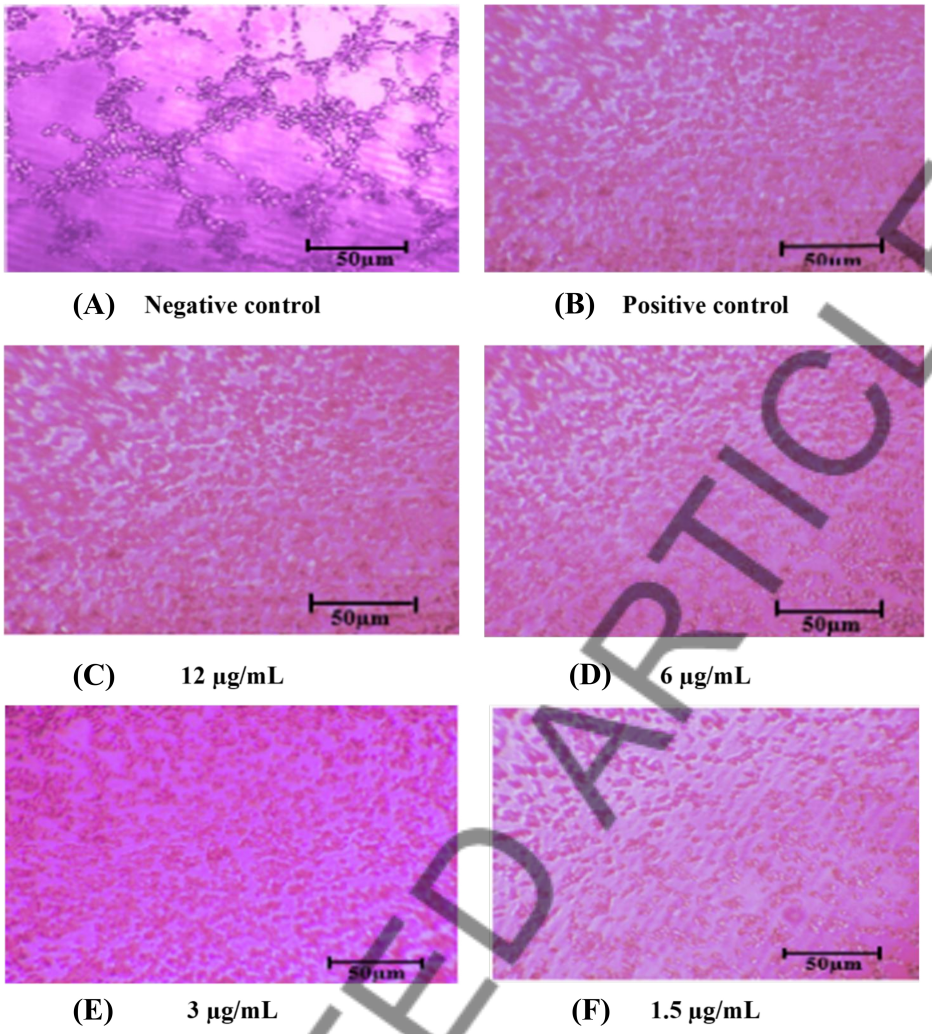


Figure 4. Inhibition of tube formation in Ea.hy926 cells following treatment with MO-AgNPs. Representative images were captured using an inverted microscope at 40× total magnification after 2.5 h of treatment. The experimental groups included: (**A**) negative control (0.05% DMSO:0.05% deionized water); (**B**) positive control (quercetin, 15.11 µg/mL); (**C**) MO-AgNPs at concentrations of 12 µg/mL; (**D**) MO-AgNPs at concentrations of 6 µg/mL; (**E**) MO-AgNPs at concentrations of 3 µg/mL; (**F**) MO-AgNPs at concentrations of 1.5 µg/mL. MO-AgNPs at 12 and 6 µg/mL markedly inhibited tube formation, showing nearly 100% inhibition when results were normalized to the negative control, demonstrating strong anti-angiogenic potential at these concentrations. Ea.hy926: endothelial cell line; MO-AgNPs: *Moringa oleifera* silver nanoparticles

Anti-tumour properties of MO-AgNPs using co-cultured 3D spheroid model

To address the need for a more complex analysis of tumor endothelial interactions, a multicellular 3D spheroid model was employed. This method simulates the physical interaction between ECs and tumor cells. In this study, the effect of MO-AgNPs at concentrations of 1.5, 3, 6, and 12 µg/mL on spheroid growth was evaluated over 14 days. Comparisons were made with a positive control (quercetin at 15.11 µg/mL) and a negative control (0.05% DMSO and 0.05% deionized water). As shown in Figure 7, spheroids were observed under an inverted microscope at 40× magnification. By day 14, a significant reduction in spheroid size was recorded in the groups treated with 6 µg/mL, 12 µg/mL MO-AgNPs, and 15.11 µg/mL quercetin (Figure 8). In contrast, the treatments at 3 and 1.5 µg/mL did not result in significant changes at any time point. Table 2 shows that the spheroid size on day 14 was reduced to 17 ± 0.158% with MO-AgNPs (12 µg/mL) and 14 ± 0.417% with quercetin. The corresponding growth inhibition rates were 83 ± 0.16% and 86 ± 0.42%, respectively (Figure 9). These findings highlight the strong inhibitory effect of MO-AgNPs at higher concentrations on tumor spheroid expansion in co-culture models.

Discussion

Previous studies have highlighted the anti-inflammatory properties of *Moringa oleifera*, largely attributed to its rich content of flavonoids, phenolic acids, and other bioactive compounds [2]. However, the anti-

RETRACTED ARTICLE

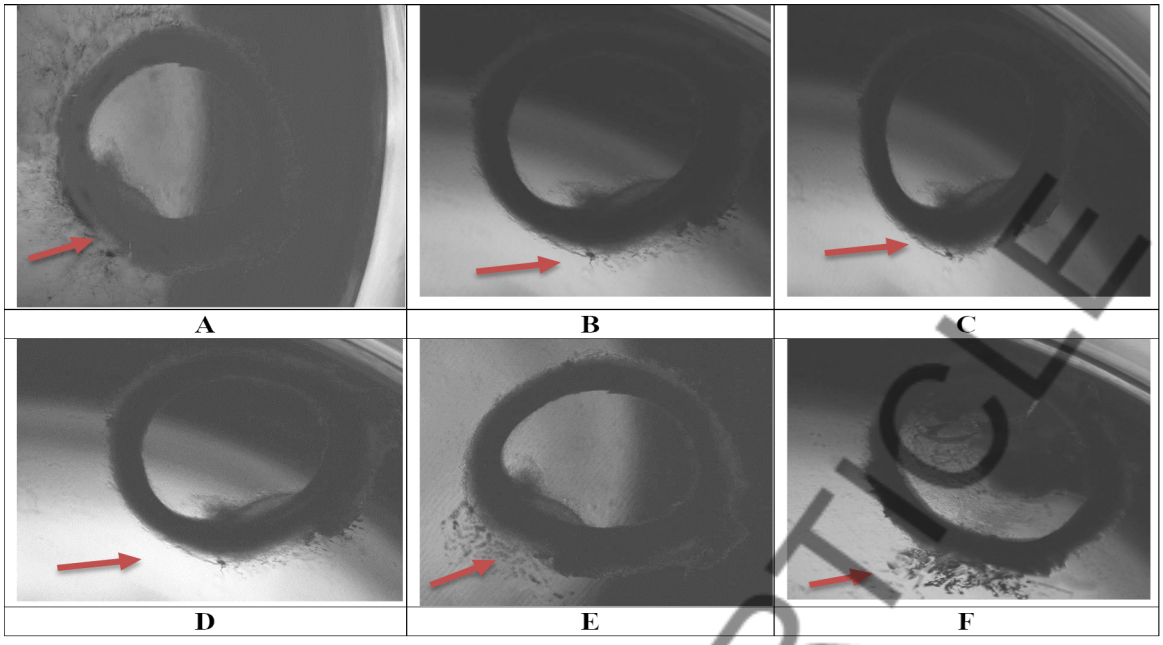


Figure 5. Inhibition of neovascularization following seven days of treatment with MO-AgNPs. Microscopic observations were conducted using an inverted microscope at 40× magnification. Treatments included: (**A**) negative control (0.05% DMSO:0.05% deionized water); (**B**) positive control (suramin, 100 µg/mL); (**C**) MO-AgNPs at concentrations of 12 µg/mL; (**D**) MO-AgNPs at concentrations of 6 µg/mL; (**E**) MO-AgNPs at concentrations of 3 µg/mL; (**F**) MO-AgNPs at concentrations of 1.5 µg/mL. Among all treatments, MO-AgNPs at 12 µg/mL exhibited significant inhibition of neovascularization. MO-AgNPs: *Moringa oleifera* silver nanoparticles

Table 1. Percentage inhibition of neovascularization following treatment with *Moringa oleifera* silver nanoparticles at 12, 6, 3, and 1.5 µg/mL concentrations, assessed using the rat aortic ring assay

Group	Percentage inhibition ± SD
100 µg/mL suramin (positive control)	70.927 ± 0.703
12 µg/mL	83.824 ± 0.081
6 µg/mL	72.065 ± 0.657
3 µg/mL	23.321 ± 0.563
1.5 µg/mL	13.599 ± 0.755

SD: standard deviation

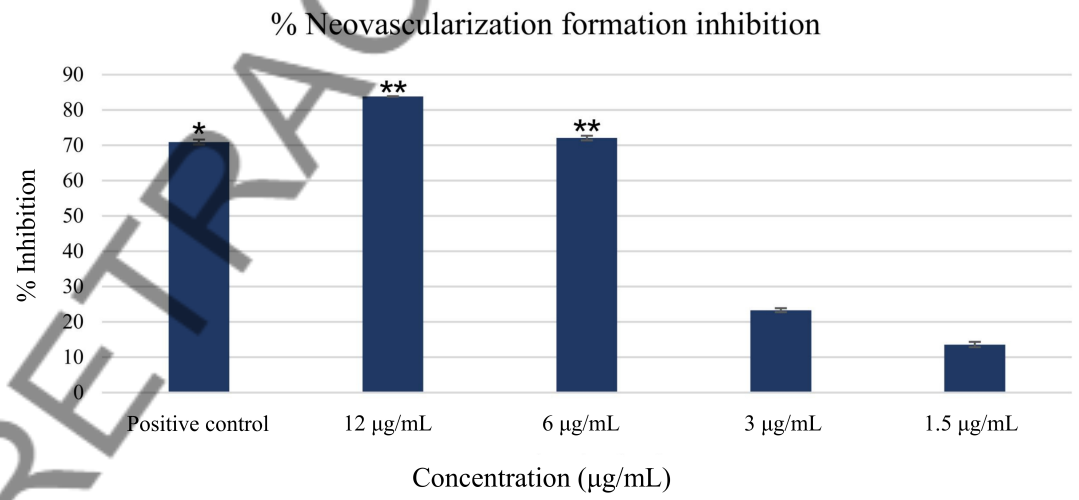


Figure 6. Percentage of neovascularization inhibition following seven-day treatment with MO-AgNPs and suramin. The graph presents the percentage inhibition of new blood vessel formation after treatment with MO-AgNPs at various concentrations, alongside a positive control group treated with suramin (100 µg/mL). Results are expressed as mean inhibition percentages relative to the negative control (0.05% DMSO:0.05% deionized water). Statistical analysis was performed using the Kruskal-Wallis test. **P*-value < 0.05, ***P*-value < 0.01 indicate statistically significant differences compared to the negative control. MO-AgNPs: *Moringa oleifera* silver nanoparticles

RETRACTED ARTICLE

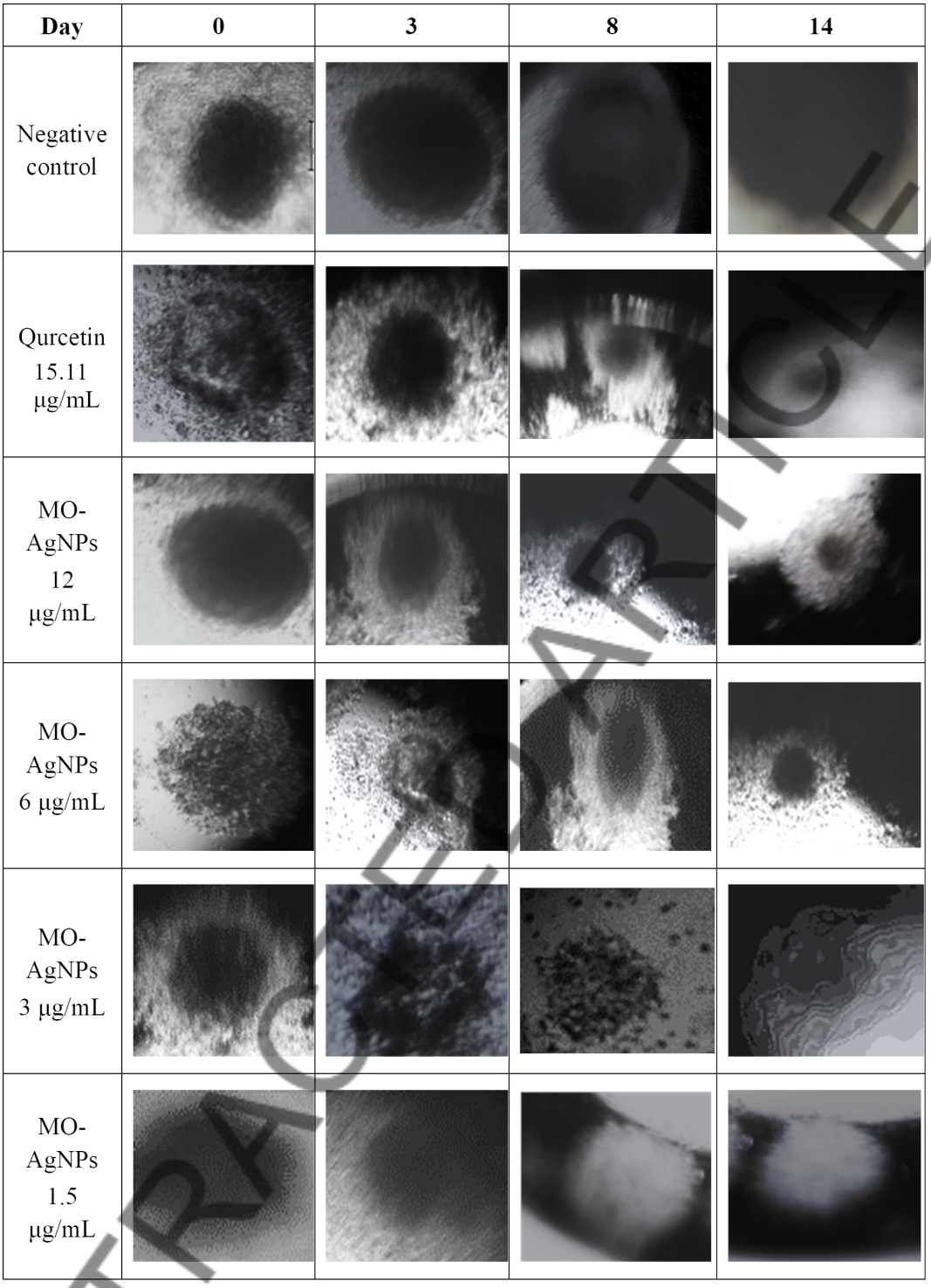


Figure 7. Growth of co-culture spheroids composed of HT29 and Ea.hy926 cell lines from day 0 to day 14, and the effect of MO-AgNPs and quercetin treatment. Spheroid formation and growth were monitored over a 14-day period. A marked inhibition of spheroid growth was observed on day 14 following treatment with MO-AgNPs at 6 µg/mL, 12 µg/mL, and quercetin at 15.11 µg/mL, compared to the untreated control. Images were taken using an inverted microscope at 40× magnification. Ea.hy926: endothelial cell line; MO-AgNPs: *Moringa oleifera* silver nanoparticles

angiogenic properties of MO-AgNPs remain relatively underexplored. In this study, MO-AgNPs demonstrated significant inhibitory effects on angiogenesis-related processes. These effects may be attributed to the ability of MO-AgNPs to interfere with key signaling pathways involved in angiogenesis-mediated responses. Bioactive compounds in *Moringa oleifera* are known to modulate oxidative stress and suppress pro-angiogenic gene expression. Similar mechanisms have been reported for other plant-derived silver nanoparticles (AgNPs), including those synthesized from *Azadirachta indica* and *Camellia sinensis*,

RETRACTED ARTICLE

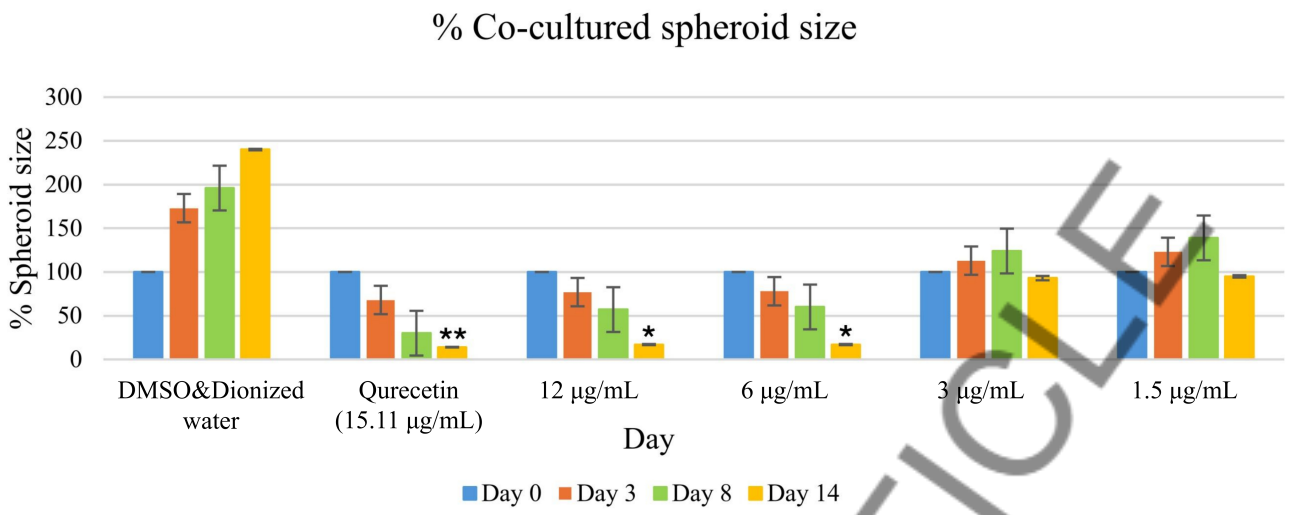


Figure 8. Size percentage of co-cultured spheroids in treated and untreated groups over a 14-day period. Spheroids composed of HT29 and Ea.hy926 cells were monitored at days 0, 3, 8, and 14 following treatment. The treated groups received MO-AgNPs at concentrations of 12, 6, 3, and 1.5 µg/mL, while the positive control was treated with quercetin (15.11 µg/mL). Spheroid size was measured and expressed as a percentage relative to day 0. A statistically significant reduction in spheroid size was observed at day 14 in the 6 µg/mL and 12 µg/mL MO-AgNP and 15.11 µg/mL quercetin groups. Statistical analysis was performed using the Kruskal-Wallis test. *P-value < 0.05, **P-value < 0.01 indicate significant differences compared to the untreated control. Ea.hy926: endothelial cell line; MO-AgNPs: *Moringa oleifera* silver nanoparticles

Table 2. Size percentage of co-cultured spheroids compared to the untreated control (0.05% DMSO:0.05% deionized water)

Size percentage of co-cultured spheroid ± SD (Normalised to the negative control)						
Day	**Negative control (µg/mL)**	**Quercetin (15.11 µg/mL)**	**MO-AgNPs (µg/mL)**			
			12	**6**	**3**	**1.5**
0	100 ± 0.852	100 ± 0.185	100 ± 1.701	100 ± 1.058	100 ± 0.341	100 ± 1.474
3	173 ± 0.843	68 ± 0.616	77 ± 0.488	78 ± 0.386	113 ± 4.311	123 ± 0676
8	196 ± 0.707	30 ± 0.141	57 ± 0.363	60 ± 1.087	124 ± 3.395	139 ± 2.366
14	240 ± 1.004	14 ± 0.417	17 ± 0.158	17 ± 0.199	93 ± 1.943	95 ± 0.894

Results are expressed as mean ± SD; SD: standard deviation; MO-AgNPs: *Moringa oleifera* silver nanoparticles

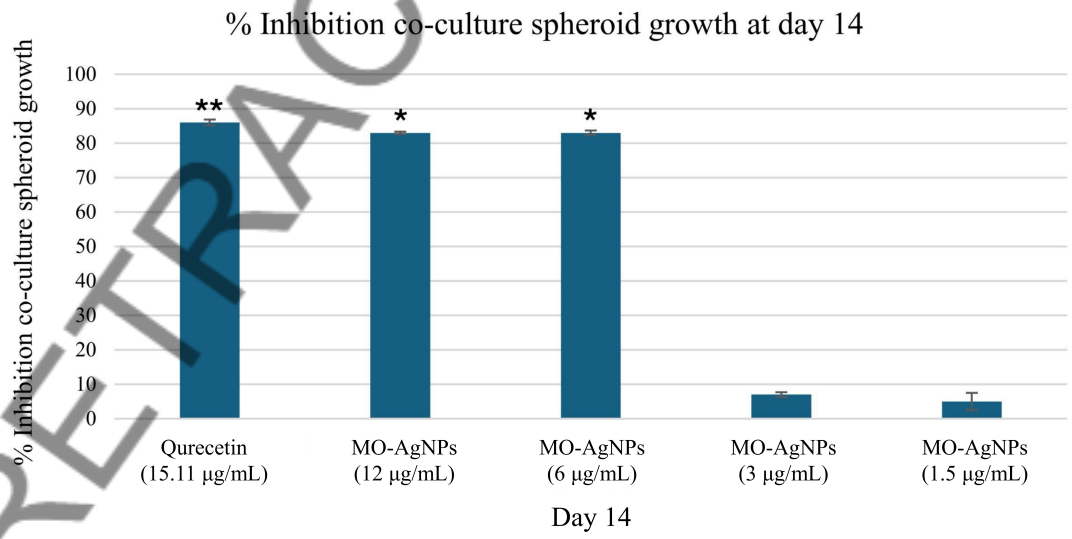


Figure 9. Percentage inhibition of co-cultured spheroid growth after 14 days of treatment with MO-AgNPs and quercetin. Spheroids composed of HT29 and Ea.hy926 cells were exposed to MO-AgNPs at concentrations of 12, 6, 3, and 1.5 µg/mL, as well as to quercetin at 15.11 µg/mL (positive control). The percentage of spheroid growth inhibition was assessed on day 14 relative to the untreated control. A significant inhibition of spheroid growth was observed following treatment with 6 µg/mL, 12 µg/mL of MO-AgNPs and 15.11 µg/mL quercetin. Statistical analysis was performed using the Kruskal-Wallis test. *P-value < 0.05, **P-value < 0.01 indicate significant differences compared to the negative control. MO-AgNPs: *Moringa oleifera* silver nanoparticles

RETRACTED ARTICLE

which also demonstrated vascular endothelial growth factor (VEGF) suppression and inhibition of EC migration. Our findings align with these reports and suggest that the synergistic action of phytochemicals and nanosilver enhances anti-angiogenic potential. Compared to chemically synthesized AgNPs, plant-based AgNPs offer a biocompatible, multifunctional platform with both carrier and therapeutic roles, making them promising candidates for integrated cancer therapies [21, 22]. In detail, treatment with MO-AgNPs at a concentration of 12 µg/mL resulted in greater inhibition of EC invasion and tube formation compared to the positive control, quercetin (15.11 µg/mL), with inhibition percentages of 62.10% and 56.70%, respectively. In contrast, lower concentrations (3 and 1.5 µg/mL) exhibited minimal inhibition, with effects closer to those of the negative control.

The ex vivo rat aortic ring assay further confirmed the anti-angiogenic potential of MO-AgNPs, with 12 µg/mL producing a higher neovascularization inhibition rate (83.824 ± 0.081%) than suramin (100 µg/mL), which showed 70.927 ± 0.703% inhibition. These findings suggest that MO-AgNPs may exert their anti-angiogenic effects by suppressing key mechanisms involved in angiogenesis, including EC proliferation, migration, and sprouting. These inhibitory effects may be linked to the presence of bioactive phytochemicals on the nanoparticle surface, which interact with angiogenic signaling pathways such as VEGF, PI3K/Akt, and MMPs, as supported by previous literature [16, 23].

Additionally, the 3D spheroid assay provided further insights into the anti-angiogenic and anti-tumor effects of MO-AgNPs. Treatment with 6 µg/mL, 12 µg/mL MO-AgNPs, and 15.11 µg/mL quercetin significantly reduced spheroid volume by day 14, compared to the untreated control. The 3D spheroid model closely mimics the tumor microenvironment, offering a more physiologically relevant system to assess the impact of therapeutic agents on tumor progression. Previous studies have shown that anti-angiogenic agents disrupt spheroid growth by interfering with cell-cell interactions, nutrient and oxygen diffusion, and hypoxia-driven signaling cascades, ultimately leading to tumor shrinkage [24, 25].

A brief comparison with earlier reports on plant-derived silver nanoparticles also supports our findings. Studies have shown that silver nanoparticles synthesized from plant extracts demonstrate anti-angiogenic properties, often mediated through oxidative stress, downregulation of VEGF expression, and inhibition of EC functions such as migration, proliferation, and tube formation [26]. Our results suggest that MO-AgNPs may act through comparable mechanisms, though the specific molecular targets warrant further investigation. Collectively, these findings underscore the therapeutic potential of MO-AgNPs as a promising anti-angiogenic and anti-invasive agent for treating angiogenesis-related diseases and cancer metastasis.

This study is limited by the absence of empty nanoparticle controls and molecular validation of angiogenesis markers. While DMSO served as a negative control, it does not isolate the effects of the nanoparticle carrier. Future research should include molecular assays such as qPCR or Western blot, and control nanoparticles to clarify the specific mechanisms of action.

Abbreviations

3D: three-dimensional

$AgNO_3$: silver nitrate

AgNPs: silver nanoparticles

ATCC: American type culture collection

DLS: dynamic light scattering

DMEM: Dulbecco's modified eagle medium

Ea.hy926: endothelial cell line

ECs: endothelial cells

IACUC: Institutional Animal Care and Use Committee

MO-AgNPs: *Moringa oleifera* silver nanoparticles

RETRACTED ARTICLE

SD: standard deviation

STR: short tandem repeat

UV-Vis: ultraviolet-visible

VEGF: vascular endothelial growth factor

Supplementary materials

The supplementary figure for this article is available at: https://www.explorationpub.com/uploads/Article/file/1002332_sup_1.pdf.

Declarations

Author contributions

RAS: Investigation, Writing—original draft, Writing—review & editing. VL and IAD: Supervision, Writing—review & editing. MK: Writing—review & editing. NAS: Conceptualization, Funding acquisition, Supervision, Validation, Writing—review & editing. All authors read and approved the submitted version.

Conflicts of interest

The authors declare that they have no conflicts of interest.

Ethical approval

The ethical approval to conduct the rat aortic ring assay for ex vivo anti-angiogenic evaluation of silver nanoparticles from *Moringa oleifera* was obtained from USM Institutional Animal Care and Use Committee (USM IACUC), [Ref: USM/IACUC/2022/(137)(1230)]. This animal study adheres to the Guide for the Care and Use of Laboratory Animals.

Consent to participate

Not applicable.

Consent to publication

Not applicable.

Availability of data and materials

The raw data supporting the conclusions of this manuscript will be made available by the authors, without undue reservation, to any qualified researcher.

Funding

This work was supported by Ministry of Higher Education Malaysia for Fundamental Research Grant Scheme, Grant number: [FRGS/1/2020/STG01/USM/03/2]. The funder had no role in study design, data collection and analysis, decision to publish, or preparation of the manuscript.

Copyright

© The Author(s) 2025.

Publisher's note

Open Exploration maintains a neutral stance on jurisdictional claims in published institutional affiliations and maps. All opinions expressed in this article are the personal views of the author(s) and do not represent the stance of the editorial team or the publisher.

RETRACTED ARTICLE

References

1. Hanachi P, Gharari Z, Sadeghinia H, Walker TR. Synthesis of bioactive silver nanoparticles with eco-friendly processes using *Heracleum persicum* stem extract and evaluation of their antioxidant, antibacterial, anticancer and apoptotic potential. J Mol Struct. 2022;1265:133325. [DOI]
2. Dzuvor CKO, Pan S, Amanze C, Amuzu P, Asakiya C, Kubi F. Bioactive components from *Moringa oleifera* seeds: production, functionalities and applications—a critical review. Crit Rev Biotechnol. 2022;42:271–93. [DOI] [PubMed]
3. Rafique S, Bashir S, Akram R, Jawaid S, Bashir M, Aftab A, et al. In vitro anticancer activity and comparative green synthesis of ZnO/Ag nanoparticles by moringa oleifera, mentha piperita, and citrus lemon. Ceram Int. 2023;49:5613–20. [DOI]
4. You WK, Schuetz TJ, Lee SH. Targeting the DLL/Notch Signaling Pathway in Cancer: Challenges and Advances in Clinical Development. Mol Cancer Ther. 2023;22:3–11. [DOI] [PubMed] [PMC]
5. Jikah AN, Edo GI. *Moringa oleifera*: a valuable insight into recent advances in medicinal uses and pharmacological activities. J Sci Food Agric. 2023;103:7343–61. [DOI] [PubMed]
6. Khor KZ, Joseph J, Shamsuddin F, Lim V, Moses EJ, Abdul Samad N. The Cytotoxic Effects of *Moringa oleifera* Leaf Extract and Silver Nanoparticles on Human Kasumi-1 Cells. Int J Nanomedicine. 2020;15: 5661–70. [DOI] [PubMed] [PMC]
7. Al-Shalabi R, Abdul Samad N, Al-Deeb I, Joseph J, Abualsoud BM. Assessment of Antiangiogenic and Cytotoxic Effects of Moringa oleifera Silver Nanoparticles Using Cell Lines. Curr Res Nutr Food S. 2024;12:196–211. [DOI]
8. Liu M, Yang J, Xu B, Zhang X. Tumor metastasis: Mechanistic insights and therapeutic interventions. MedComm (2020). 2021;2:587–617. [DOI] [PubMed] [PMC]
9. Banerjee S, Lo WC, Majumder P, Roy D, Ghorai M, Shaikh NK, et al. Multiple roles for basement membrane proteins in cancer progression and EMT. Eur J Cell Biol. 2022;101:151220. [DOI] [PubMed]
10. Justus CR, Marie MA, Sanderlin EJ, Yang LV. Transwell In Vitro Cell Migration and Invasion Assays. Methods Mol Biol. 2023;2644:349–59. [DOI] [PubMed] [PMC]
11. Favara DM, Liebscher I, Jazayeri A, Nambiar M, Sheldon H, Banham AH, et al. Elevated expression of the adhesion GPCR ADGRL4/ELTD1 promotes endothelial sprouting angiogenesis without activating canonical GPCR signalling. Sci Rep. 2021;11:8870. [DOI] [PubMed] [PMC]
12. Paro MR, Chakraborty AR, Angelo S, Nambiar S, Bulsara KR, Verma R. Molecular mediators of angiogenesis and neurogenesis after ischemic stroke. Rev Neurosci. 2022;34:425–42. [DOI] [PubMed] [PMC]
13. Rahman HS, Tan BL, Othman HH, Chartrand MS, Pathak Y, Mohan S, et al. An Overview of *In Vitro*, *In Vivo*, and Computational Techniques for Cancer-Associated Angiogenesis Studies. Biomed Res Int. 2020;2020:8857428. [DOI] [PubMed] [PMC]
14. Aplin AC, Nicosia RF. The Rat Aortic Ring Model of Angiogenesis. Methods Mol Biol. 2015;1214: 255–64. [DOI] [PubMed]
15. Nicosia RF. The aortic ring model of angiogenesis: a quarter century of search and discovery. J Cell Mol Med. 2009;13:4113–36. [DOI] [PubMed] [PMC]
16. Obaid KA. Anti-angiogenesis efficacy of the aqueous extract of *Allium sativum* and its combination with melatonin in an animal model: *in vivo* and *ex vivo* studies. Pharmacia. 2024;71:1–8. [DOI]
17. Kapoor A, Chen CG, Iozzo RV. A simplified aortic ring assay: A useful *ex vivo* method to assess biochemical and functional parameters of angiogenesis. Matrix Biol Plus. 2020;6–7:100025. [DOI] [PubMed] [PMC]
18. Teixeira Polez R, Huynh N, Pridgeon CS, Valle-Delgado JJ, Harjumäki R, Österberg M. Insights into spheroids formation in cellulose nanofibrils and Matrigel hydrogels using AFM-based techniques. Mater Today Bio. 2024;26:101065. [DOI] [PubMed] [PMC]

RETRACTED ARTICLE

19. Zámková M, Prokop M, Stolín R. Non-Parametric Anova Methods Applied on Students' Performance Development in Course of Statistics. Acta Univ Agric Silvic Mendelianae Brun. 2020;68:281–9. [DOI]
20. Almatroodi SA, Alsahli MA, Aljohani ASM, Alhumaydhi FA, Babiker AY, Khan AA, et al. Potential Therapeutic Targets of Resveratrol, a Plant Polyphenol, and Its Role in the Therapy of Various Types of Cancer. Molecules. 2022;27:2665. [DOI] [PubMed] [PMC]
21. Kitimu SR, Kirira P, Abdille AA, Sokei J, Ochwang'i D, Mwitari P, et al. Anti-Angiogenic and Anti-Metastatic Effects of Biogenic Silver Nanoparticles Synthesized Using *Azadirachta indica*. Adv Biosci Biotechnol. 2022;13:188–206. [DOI]
22. Subramaniam P, Nisha KMJ, Vanitha A, Kiruthika ML, Sindhu P, Elesawy BH, et al. Synthesis of silver nanoparticles from wild and tissue cultured *Ceropegia juncea* plants and its antibacterial, anti-angiogenesis and cytotoxic activities. Appl Nanosci. 2023;13:1619–33. [DOI]
23. Majnooni MB, Fakhri S, Ghanadian SM, Bahrami G, Mansouri K, Iranpanah A, et al. Inhibiting Angiogenesis by Anti-Cancer Saponins: From Phytochemistry to Cellular Signaling Pathways. Metabolites. 2023;13:323. [DOI] [PubMed] [PMC]
24. Carvalho S, Silveira MJ, Domingues M, Ferreira B, Pereira CL, Gremião MP, et al. Multicellular Quadruple Colorectal Cancer Spheroids as an In Vitro Tool for Antiangiogenic Potential Evaluation of Nanoparticles. Adv Ther. 2023;6:2200282. [DOI]
25. Ahn J, Kim DH, Koo DJ, Lim J, Park TE, Lee J, et al. 3D microengineered vascularized tumor spheroids for drug delivery and efficacy testing. Acta Biomater. 2023;165:153–67. [DOI] [PubMed]
26. Rama P, Baldelli A, Vignesh A, Altemimi AB, Lakshmanan G, Selvam R, et al. Antimicrobial, antioxidant, and angiogenic bioactive silver nanoparticles produced using *Murraya paniculata* (L.) jack leaves. Nanomater Nanotechno. 2022;12:1–10. [DOI]

RETRACTED ARTICLE